ADVANCED MATERIALS

Large-Scale Synthesis of Rings of Bundled Single-Walled Carbon Nanotubes by Floating Chemical Vapor Deposition**

By *Li Song, Lijie Ci, Lianfeng Sun, Chuanhong Jin, Lifeng Liu, Wenjun Ma, Dongfang Liu, Xiaowei Zhao, Shudong Luo, Zengxing Zhang, Yanjuan Xiang, Jianjun Zhou, Weiya Zhou, Yong Ding, Zhonglin Wang*, and *Sishen Xie**

Since their discovery,[1] single-walled carbon nanotubes (SWNTs) have attracted considerable attention due to their unique chemical and physical properties, as well as their promise in the area of materials chemistry.[2] Using previously reported synthetic methods, carbon nanotubes (CNTs) are always grown as long strings, and this string shape largely determines their properties. CNTs with annular geometries make for rather unusual superstructures, and these closed-ring systems have been found to exhibit interesting transport properties.[3,4] Recently, several post-treatment methods, including chemical modification and physical treatment, have been developed to fabricate nanotube rings. Using ultrasonic irradiation, Avouris and co-workers have found that linear CNTs can be folded into nanotube rings with various diameters.[5] Sano et al.[6] have used covalent ring-closure reactions to produce a sizeable number of nanotube rings from etched straight nanotubes. Meanwhile, SWNT rings have also been accidentally observed in directly synthesized materials. Liu et al.[7] have detected trace quantities of rings (0.01–0.1 %) by scanning force and transmission electron microscopy (TEM) in raw SWNT samples made by laser ablation. There has also been a report of SWNT rings formed by solvent evaporation.[8] Most recently, a small number of double-walled carbon nanotube rings have been identified in the products of a solid-solution reaction.[9] However, if these nanotube rings are to be used for practical applications, a key issue that needs to be resolved is their large-scale synthesis with high purity.

In this paper, bundles of SWNT rings have been synthesized in high yields by thermally decomposing acetylene at 1100 °C in a floating iron catalyst system. The rings typically have a small average diameter with a narrow size distribution and appear to mostly consist of SWNT toroids. The rings can be deposited on different substrates with varying densities at relatively low temperatures, which is a significant advantage for potential applications such as electronic devices. Raman scattering indicates that the Raman G-mode of the SWNT rings is split into several peaks over a broad frequency range, which can be ascribed to the bending strain of SWNT bundles induced by the curvature of the ring. The synthesis of SWNT rings reported here paves the way for investigating transport, electronic, and optical phenomena in these annular nanotube structures.

The typical morphology of the nanotube rings is shown in Figure 1. Figure 1a clearly illustrates the high yield of nanotube rings synthesized by the optimized floating chemical vapor deposition (CVD) method. From many scanning electron microscopy (SEM) images of the products, we estimate that the yield of the grown rings is greater than 70 %, which greatly surpasses the yields previously achieved by other direct-growth techniques. Also, we observe that some of the rings fall on the substrate, while others adhere to the edge. The SEM image in Figure 1b shows that these structures have a well-defined ring configuration. The rings typically have an average diameter of 120 nm and a narrow thickness distribution ranging from 15 to 30 nm, as shown in Figure 1c and d, respectively. It is worth noting that the diameter of the SWNT rings here is much smaller than the previously reported diameters of 300–500 nm observed for rings synthesized by laser ablation and 500–600 nm seen for post-treated nanotube solutions.[6,7] The smaller diameter of the rings may lead to more interesting quantum effects and electronic properties.[3,4]

[*] Prof. S. Xie, Dr. L. Song, Dr. C. Jin, Dr. L. Liu, Dr. W. Ma, Dr. D. Liu, Dr. X. Zhao, Dr. S. Luo, Dr. Z. Zhang, Dr. Y. Xiang, Dr. J. Zhou, Prof. W. Zhou
Beijing National Laboratory for Condensed Matter Physics
Institute of Physics
Chinese Academy of Science
Beijing 100080 (P.R. China)
E-mail: ssxie@aphy.iphy.ac.cn
Dr. L. Song, Dr. C. Jin, Dr. L. Liu, Dr. W. Ma, Dr. D. Liu, Dr. X. Zhao, Dr. S. Luo, Dr. Z. Zhang, Dr. Y. Xiang
Graduate School of Chinese Academy of Sciences
Chinese Academy of Science
Beijing 100039 (P.R. China)
Dr. L. J. Ci
Max Planck Institut fuer Metallforschung
Stuttgart 70569 (Germany)
Prof. L. F. Sun
National Centre for Nanoscience and Nanotechnology
Beijing 100080 (P.R. China)
Dr. Y. Ding, Prof. Z. L. Wang
School of Materials Science and Engineering
Georgia Institute of Technology
Atlanta, GA 30332-0245 (USA)

© 2006 WILEY-VCH Verlag GmbH & Co. KGaA, Weinheim
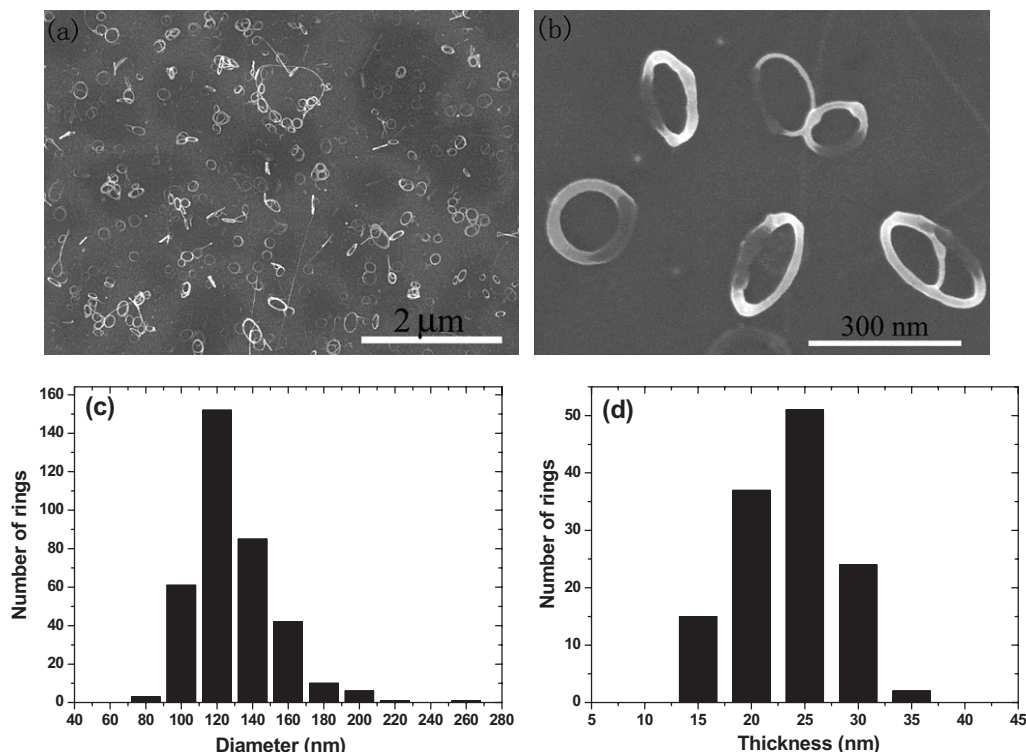
Figure 1. a) Low- and b) high-magnification SEM images of SWNT rings deposited on a silicon substrate. The nanotube rings are clearly visible. Histograms showing the c) diameter distribution and d) thickness distribution of the rings.

The growth process has been studied as a function of various experimental parameters in order to obtain optimal synthesis conditions. Among these factors, the amount of sublimed catalyst, which can be adjusted by changing the sublimation temperature, seems to play the most important role in determining the proportion of SWNT rings in the as-grown products. With an increase in the sublimation temperature from 50 to 65 °C, more of the catalyst is sublimed, and the samples tend to have proportionately more SWNTs with a linear structure. Conversely, when the sublimation temperature is below 50 °C, neither ring nor linear SWNT products are obtained. Meanwhile, it has been found that the reactant gas flow greatly influences the formation of SWNT rings. The optimum flow ranges from 200 to 600 sccm with the ratio of acetylene to argon varying from about 0.02 to 0.1 vol %. Further, we find that the quantity of SWNT rings obtained is also influenced by other experimental parameters, such as the reaction time and the growth temperature. Therefore, by adjusting these parameters, we can deposit SWNT rings onto different substrates with a wide range of densities, as demonstrated in Figure 2. This represents a major advantage for developing nanotube-ring-based nanoelectronics.[2,10]

The nanotube rings were also deposited on a copper grid for TEM characterization. Figure 3a shows a typical TEM image of two rings. It appears that the annular rings are composed of SWNT bundles decorated with very small diameter nanoparticles. The nanoparticles in the rings are iron
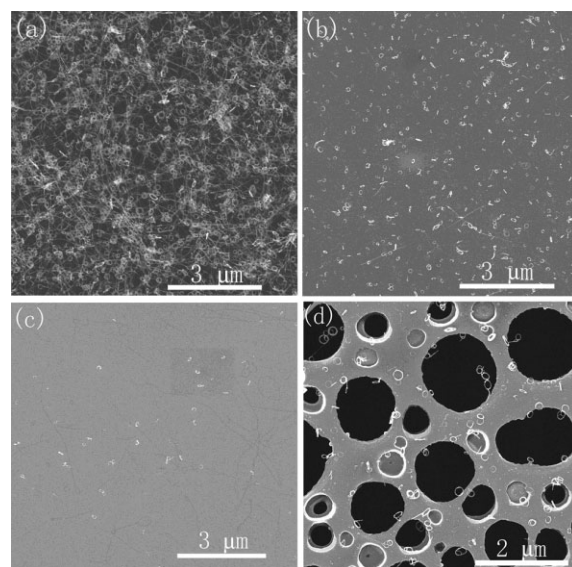
Figure 2. SEM images of SWNT rings with different nanotube densities deposited on a–c) a silicon substrate and d) a copper substrate.

catalysts encapsulated by several graphite layers, as confirmed by energy dispersive X-ray (EDX) spectroscopy. The atomic layer fringes corresponding to individual tubes forming the bundle are clearly visible in Figure 3a. The thickness of the ring is 25 nm. Furthermore, the structure appears to be a perfect torus with no clear evidence of a beginning or end. When
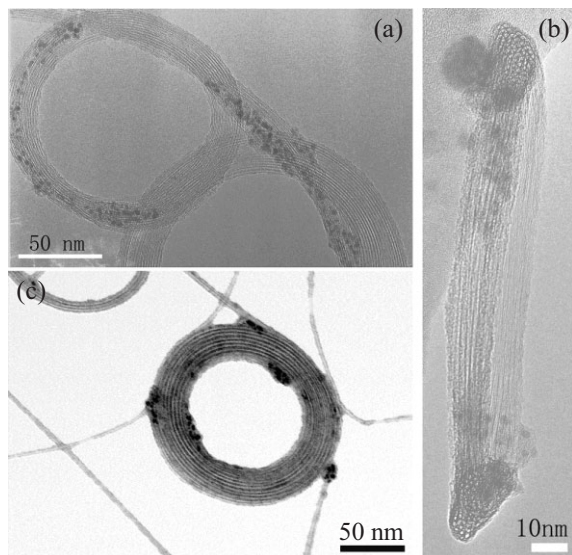
Figure 3. a) High-resolution TEM (HRTEM) image of two SWNT rings adhering to each other. b) HRTEM cross-sectional view of a SWNT ring. c) TEM images of a SWNT ring supported by several linear nanotubes.

the plane of the ring is nearly parallel to the incident electron beam, we can observe the cross section of the ring, as shown in Figure 3b. The high-resolution TEM (HRTEM) image of the cross section of a ring confirms that SWNTs with diameters of 1 to 2 nm are tightly packed within the rings. The SWNTs appear to be stacked in a close-packed hexagonal arrangement.

Micro-Raman spectroscopy can be effectively employed to study the properties of SWNTs.[11] Figure 4 shows micro-Raman spectra for as-grown SWNT rings, measured at a laser excitation wavelength of 532 nm (2.33 eV). The Raman spectra consist of two main groups of peaks. The first group, consisting of peaks at 122, 157, and 190 cm^{-1}, correspond to the radial breathing modes (RBMs), with frequencies dependent on
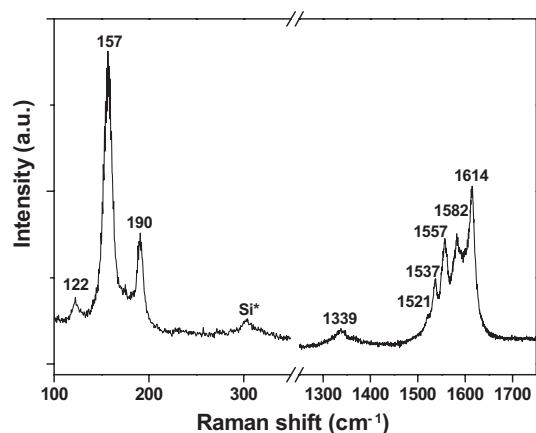
Figure 4. Raman spectra of SWNT rings deposited on a silicon substrate. The peak indicated by an asterisk arises from the silicon substrate.
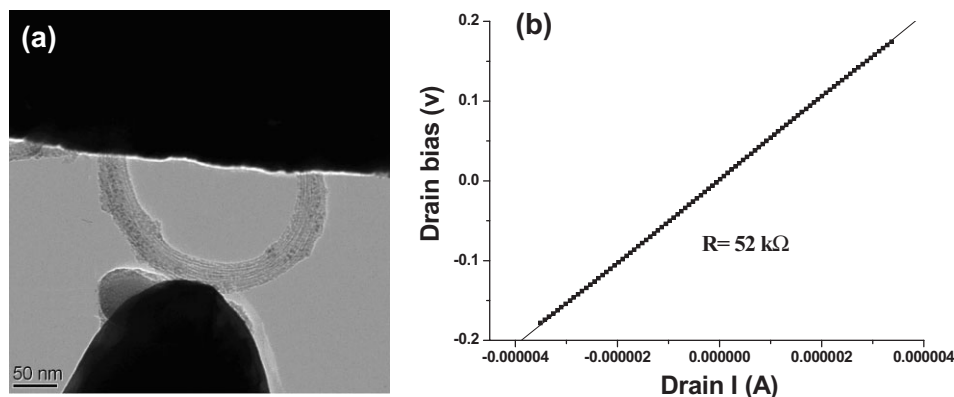
the diameter of the SWNTs. According to the relationship between the diameter (d) and the frequency (ω)

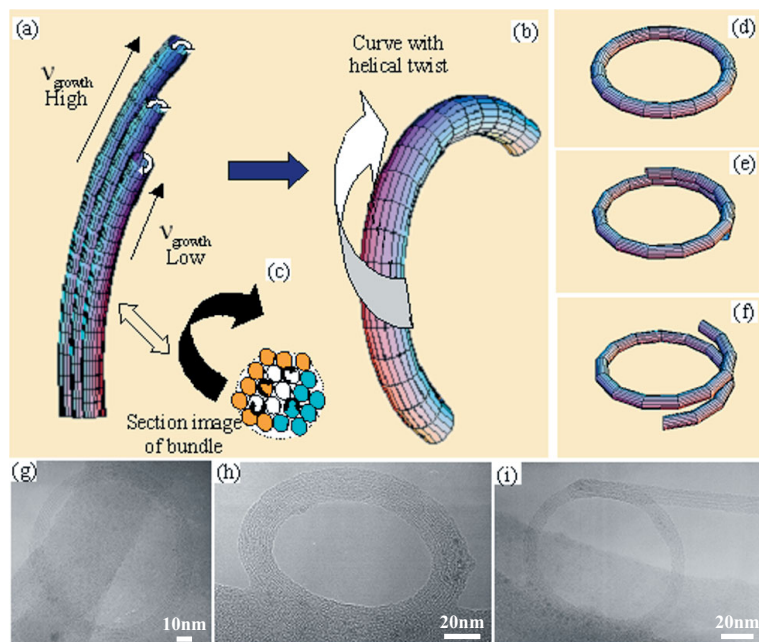$$\omega_{\mathrm{RBM}} = 224/d + 10 \ [\mathrm{nm}] \qquad (1)^{[12]}$$

the Raman peaks at 122, 157, and 190 cm^{-1} correspond to diameters of 2.0, 1.52, and 1.24 nm, which is consistent with the TEM observations. Based on the relationship between the diameter and chirality of SWNTs,[2] we have determined that nanotubes with different symmetries are present inside the ring bundles, including armchair, zigzag, and other helical nanotubes. The sharp peak at 157 cm^{-1} arises from the resonance enhancement of the Raman signal.[13] In the second group of peaks at higher frequencies, we observe peaks at 1521, 1537, 1557, 1582, and 1614 cm^{-1}, which are related to the G tangential stretching modes of the SWNTs. It is worth noting that the Raman G-modes of the SWNT rings are split into several peaks at different positions, which is quite different from the previously observed G-modes of the linear SWNTs.[11] According to early studies, the Raman G-mode of large-diameter (> 1 nm) SWNTs is not typically characterized by so many peaks spread over a broad range of Raman frequencies. Here, the annular geometry of the SWNT ring induces a change in the C–C bond conformation along the circumference of the ring, leading to uniaxial C–C bond elongation and compression. Previous studies of SWNTs have shown that a down-shift of the Raman G-mode is observed for SWNTs upon the application of an uniaxial strain, while an up-shift is observed under hydrostatic pressure.[14,15] Consequently, the splitting behavior observed here is tentatively ascribed to bending strains resulting from the coiling-induced curvature of the nanotube rings. Strain-induced shifts of the Raman peaks likely lead to the observed splitting of the G-mode over a broad range of frequencies. Additionally, the intertube interactions between individual SWNTs in the bundles may also affect the splitting of the Raman G-mode of these rings.[12] The D-band around 1339 cm^{-1} can be attributed to defects in the nanotubes or amorphous carbon in the sample.

We have measured the electronic properties of the SWNT rings using an in situ TEM system at room temperature. The details of the measurement setup have been reported previously.[16] Figure 5a shows that a SWNT ring was connected between the W tip and the Pt electrodes. The corresponding current–voltage (*I*–*V*) curve is shown in Figure 5b. The resistance of the ring was determined to be 52 kΩ, which is similar to values reported previously.[17] Further studies are planned to investigate the electronic characteristics of the SWNT rings under an applied magnetic field and at low temperatures, which should be helpful for understanding interesting physical phenomena such as the Aharonov–Bohm effect.[18]

There are several plausible mechanisms which could lead to the formation of SWNT rings.[5,7,19] Based on our TEM and SEM results, we attribute the formation of the rings to the curling and attachment of SWNTs. A simple schematic model of the growth process is shown in Figure 6. As is well known,

ADVANCED MATERIALS

Figure 5. The two-terminal resistance of a SWNT ring has been measured at room temperature using an in situ TEM system. a) TEM image showing the W tip, the SWNT ring, and the Pt electrodes; b) the corresponding *I–V* plot.

suggesting that SWNT bundles can be induced to curl up into curved shapes due to the mismatch between growth rates among different tubes in the same bundle; the tubes curve to relieve the stress energy arising from intertube interactions (Fig. 6a–c). Furthermore, according to our experimental results, perturbed regions in the vapor stream and the density of bundles may have an effect on the curving process. After having formed curved structures, the bundles may be coherently attached to each other by van der Waals interactions. When the two ends of a tube adhere to the sidewall of a bundle and are attached to each other, the bundles show a toroidal shape, and the ends of the bundles can be observed (Fig. 6d–f). These possible forms have been confirmed by TEM images of SWNT rings in our experiments, as shown in Figure 6g–i. A balance between tube–tube Van der Waals adhesion and the strain energy resulting from coiling-induced curvature is thought to produce the stable nanotube ring structures.[5,23]

In summary, we have demonstrated a new process for the large-scale growth of SWNT rings in high yields by thermally decomposing C_2H_2 in a floating iron catalyst system. The rings typically have a diameter of 120 nm. The Raman spectra and electrical properties of the rings have been measured. The rings can be deposited with widely varying densities on many different substrates at low temperatures, which is a remarkable advantage for potential applications such as electronic devices. This low-temperature deposition process allows for the integration of the rings with silicon and microelectromechanical systems technology. The synthesis method of SWNT rings reported here paves the way for the investigation of transport phenomena through annular nanotube structures and will provide promising materials for building nanoscale electronic circuits.

Figure 6. Schematic depiction of the ring growth mechanism. The cylinder corresponds to a SWNT bundle. a,b) The bundles are induced to twist and bend by the varying growth stress for different nanotubes and due to the tube–tube interactions. c) Schematic depiction of a cross section of SWNT bundles showing the varying growth rates of the nanotubes and the SWNTs twisting against one another. d–f) Possible shapes of bundles resulting from the curling process, compared with g–i) TEM images of SWNT rings observed in our experiments.

SWNTs in bundles grow with different growth rates due to the different extrusion velocities of carbon atoms on the catalyst.[20] We believe that the SWNT bundles curve due to the growth-induced stress between the outer and inner nanotubes inside the bundles. This causes the different nanotube chiralities to twist against one another.[21] As a result, the bundle may willingly bend to form a curved shape in order to release the stress energy resulting from the interactions between the nanotubes, analogous to the coiling and ring formation of bio-polymers such as DNA and proteins.[22] Essentially, we are

Experimental

The experimental setup consisted of a two-stage furnace system fitted with a special quartz-tube structure. A quartz tube with a diameter of 10 mm was embedded in an outer quartz tube (inner diameter of 30 mm), as shown in Figure 7. Ferrocene (bis(cyclopentadienyl) iron) mixed with sulfur was used as the catalyst source. The catalyst was sublimed at a temperature of 50–65 °C and carried by a flowing argon (200–600 sccm) and acetylene (1–3 sccm) mixture into a second
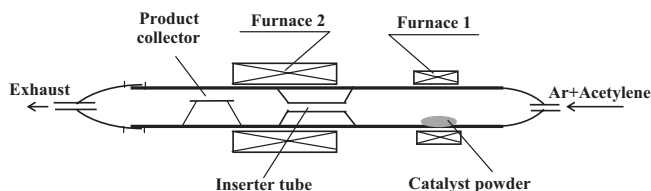
Figure 7. Schematic depiction of the floating catalyst CVD setup for preparing SWNT rings.

furnace through the small inserted quartz tube. The reaction temperature of the second furnace was 1100 °C and the system pressure was held at 1 atm (1 atm = 10 133 Pa). After a growth period of 30 min, the as-grown products were collected using different substrates placed at low-temperature (200–300 °C) regions, such as copper grids, positive silicon, and silicon oxide wafers.

SEM (S-5200), TEM (T-20), and micro-Raman spectroscopy (Renishaw TY-64000) were used to characterize the as-grown SWNT rings. The electronic properties of the SWNT rings were tested using an in situ TEM system at room temperature.

[1] S. Iijima, T. Ichihashi, *Nature* **1993**, *363*, 603.
[2] a) B. Yakobson, R. E. Smalley, *Am. Sci.* **1997**, *85*, 324. b) C. Dekker, *Phys. Today* **1999**, *52*, 22. c) R. Saito, M. S. Dresselhaus, *Physical Properties of Carbon Nanotubes*, Imperial College Press, London **1998**.
[3] R. C. Haddon, *Nature* **1997**, *388*, 31.
[4] S. Latil, S. Roche, A. Rubio, *Phys. Rev. B: Condens. Matter* **2003**, *67*, 165 420.
[5] a) R. Martel, H. R. Shea, Ph. Avouris, *Nature* **1999**, *398*, 299. b) R. Martel, H. R. Shea, Ph. Avouris, *J. Phys. Chem. B* **1999**, *103*, 7551.
[6] M. Sano, A. Kamino, A. Okamura, S. Shinkai, *Science* **2001**, *293*, 1299.
[7] J. Liu, H. J. Dai, J. H. Hafner, D. T. Colbert, R. E. Smalley, S. J. Tans, C. Dekker, *Nature* **1997**, *385*, 780.
[8] a) P. McEuen, personal communication. b) T. Vossmeyer, S.-W. Chung, W. M. Gelbart, J. R. Heath, *Adv. Mater.* **1998**, *10*, 351.
[9] a) J.-F. Colomer, L. Henrard, E. Flahaut, G. Van Tendeloo, A. A. Lucas, Ph. Lambin, *Nano Lett.* **2003**, *3*, 685. b) E. Flahaut, A. Peigney, Ch. Laurent, A. Rousset, *J. Mater. Chem.* **2000**, *10*, 249.
[10] T. Rueckes, K. Kim, E. Joselevich, G. Tseng, C. Cheung, C. M. Lieber, *Science* **2000**, *289*, 94.
[11] A. M. Rao, E. Richter, S. Bandow, B. Chase, P. C. Eklund, K. A. Williams, S. Fang, K. R. Subbaswamy, M. Menon, A. Thess, R. E. Smalley, G. Dresselhaus, M. S. Dresselhaus, *Science* **1997**, *275*, 187.
[12] A. M. Rao, J. Chen, E. Richter, U. Schlecht, P. C. Eklund, R. C. Haddon, U. D. Venkateswaran, Y. K. Kwon, D. Tománek, *Phys. Rev. Lett.* **2001**, *86*, 3895.
[13] R. Saito, G. Dresselhaus, M. S. Dresselhaus, *Phys. Rev. B: Condens. Matter* **2000**, *61*, 2981.
[14] S. B. Cronin, A. K. Swan, M. S. Ünlü, B. B. Goldberg, M. S. Dresselhaus, M. Tinkham, *Phys. Rev. Lett.* **2004**, *293*, 167 401.
[15] U. D. Venkateswaran, E. A. Brandsen, U. Schlecht, A. M. Rao, E. Richter, I. Loa, K. Syassen, P. C. Eklund, *Phys. Status Solidi B* **2001**, *233*, 225.
[16] a) C. H. Jin, J. Y. Wang, M. S. Wang, J. Su, L. M. Peng, *Carbon* **2005**, *43*, 1026. b) R. Lohmus, D. Erts, A. Lohmus, K. Svensson, Y. Jompol, H. Olin, *Phys. Low-Dimens. Struct.* **2001**, *3*, 81.
[17] a) H. R. Shea, R. Martel, Ph. Avouris, *Phys. Rev. Lett.* **2000**, *84*, 4441. b) H. Watanabe, C. Manabe, T. Shigematsu, M. Shimizu, *Appl. Phys. Lett.* **2001**, *78*, 2928.
[18] a) L. A. Chernozatonskii, *Phys. Lett. A* **1992**, *172*, 173. b) D. Grimm, R. B. Muniz, A. Latgé, *Phys. Rev. B: Condens. Matter* **2003**, *68*, 193 407.
[19] a) O. Hod, E. Rabani, R. Baer, *Phys. Rev. B: Condens. Matter* **2003**, *67*, 195 408. b) P. B. László, I. M. Géza, A. K. Antal, J. B. Nagy, P. Lambin, *Phys. Rev. B: Condens. Matter* **2002**, *66*, 165 405.
[20] a) S. Amelinckx, X. B. Zhang, D. Bernaerts, X. F. Zhang, V. Ivanov, J. B. Nagy, *Science* **1994**, *265*, 635. b) S. Ihara, S. Itoh, J. Kitahami, *Phys. Rev. B: Condens. Matter* **1993**, *48*, 5643.
[21] a) Z. C. Ou-Yang, Z. B. Su, C. L. Wang, *Phys. Rev. Lett.* **1997**, *78*, 4055. b) S. L. Zhang, *Phys. Rev. B: Condens. Matter* **2002**, *65*, 235 411. c) A. Szabó, A. Fonseca, J. B. Nagy, Ph. Lambin, L. P. Biró, *Carbon* **2005**, *43*, 1628.
[22] a) J. W. Bryson, S. F. Betz, H. S. Lu, D. J. Suich, H. X. Zhou, K. T. O'Niel, W. F. Degrado, *Science* **1995**, *270*, 935. b) G. M. Whitesides, J. P. Mathias, C. T. Seto, *Science* **1991**, *254*, 1312. c) T. E. Creighton, *Protein Folding*, Freeman, New York **1992**.
[23] a) S. L. Zhang, S. M. Zhao, M. G. Xia, E. H. Zhang, T. Xu, *Phys. Rev. B: Condens. Matter* **2003**, *68*, 245 419. b) B. I. Yakobson, C. J. Brabec, J. Bernholc, *Phys. Rev. Lett.* **1996**, *76*, 2511. c) J. Tersoff, R. S. Ruoff, *Phys. Rev. Lett.* **1994**, *73*, 676.